

DYNAMICAL MODEL AND EIGENVALUES OF THE TURBOCHARGER

Vladimír Zeman, Zdeněk Hlaváč*

The paper deals with derivation of the dynamical model of the turbochargers with rotor supported on the two floating ring bearings. The model respects the bearing forces acting upon the journals and floating bearing rings by means of inner and outer oil-films. The gyroscopic effects, external and internal damping of the flexible rotor shaft and the rigid turbine and compressor wheels are respected. The modal analysis and the Campbell diagram is used in the turbocharger linearized model to find the critical speeds.

Keywords: turbocharger vibrations, eigenvalues, Campbell diagram, critical speeds

1. Introduction

The automotive turbochargers work at very high rotor speeds. Therefore the turbocharger vibrations caused by the rotor unbalance is fundamental phenomenon influencing a turbocharger operation. Consider the very high-speed automotive turbocharger [6] including the flexible rotor shaft (R), rigid turbine (T) and compressor (C) wheels and two cylindrical floating ring bearings (B_a , B_b) displayed in Fig. 1. The lateral-bending behaviour of the isotropic flexible rotor shaft with fixed rigid disks supported on non-isotropic bearings can be modelled by 1-D approach using the finite element method in a fixed coordinate system [4], [3], [7]. The forces transmitted by oil-film bearings can be described for small displacements from static equilibrium position by linearized stiffness and damping matrices depending on the angular rotor velocity ω . Other external and internal damping effects are neglected or are respected approximately. Mostly external vs. internal damping was studied on the fundamental model with rotor mass concentrated in the disk without [2], [4] or with

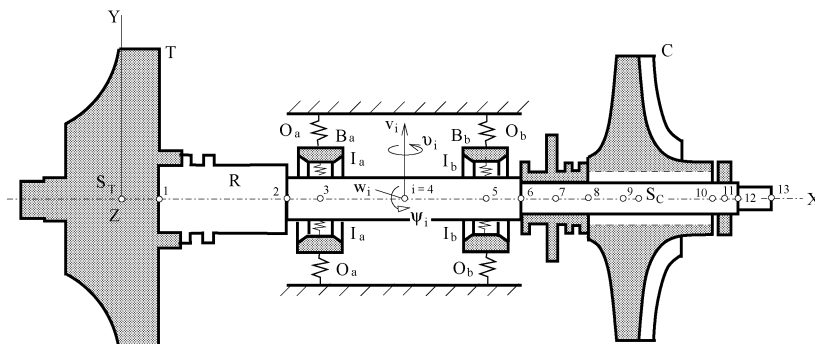


Fig.1: Computational model of the turbocharger rotor

* prof. Ing. V. Zeman, DrSc., doc. RNDr. Z. Hlaváč, CSc., University of West Bohemia, Faculty of Applied Sciences, Univerzitní 8, 306 14 Plzeň

gyroscopic effects [5]. The aim of this article is to present a generally accepted methodology for modelling of the turbocharger rotor supported on two flexible non-isotropic oil-film floating ring bearings respecting two separable oil-films of both bearings and an external and internal rotor damping.

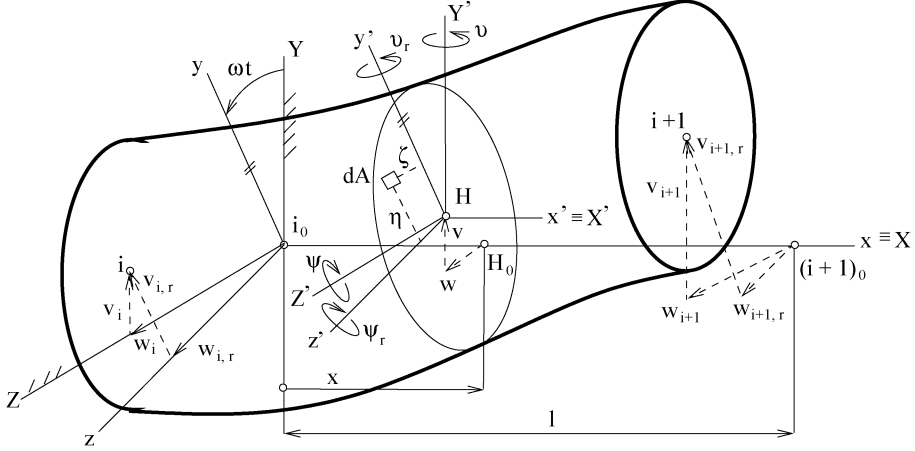


Fig.2: Prismatic shaft finite element

2. Discretization of the rotor shaft

The finite element method (FEM) is applied for a discretization of the flexible rotor shaft with rigid disks. The motion equations can be written in the space of general coordinates

$$\mathbf{q}_R = [\dots, v_i, w_i, \vartheta_i, \psi_i, \dots]^T, \quad (1)$$

where v_i , w_i are lateral and ϑ_i , ψ_i angular shaft displacements in the nodal point i in the inertial coordinate system X, Y, Z (Fig. 2). The mass $\mathbf{M}^{(e)}$, gyroscopic $\omega \mathbf{G}^{(e)}$ and stiffness $\mathbf{K}^{(e)}$ matrices of the undamped prismatic shaft finite element (FE) between two adjacent nodal points i and $i + 1$ can be derived using Lagrange's approach from the identity

$$\frac{d}{dt} \left(\frac{\partial E_k^{(e)}}{\partial \dot{\mathbf{q}}_{YZ}^{(e)}} \right) - \frac{\partial E_k^{(e)}}{\partial \mathbf{q}_{YZ}^{(e)}} + \frac{\partial E_p^{(e)}}{\partial \mathbf{q}_{YZ}^{(e)}} = \mathbf{M}^{(e)} \ddot{\mathbf{q}}_{YZ}^{(e)} + \omega \mathbf{G}^{(e)} \dot{\mathbf{q}}_{YZ}^{(e)} + \mathbf{K}^{(e)} \mathbf{q}_{YZ}^{(e)}, \quad (2)$$

where shaft FE displacements in the inertial coordinate system are arranged into vector

$$\mathbf{q}_{YZ}^{(e)} = [v_i, \psi_i, v_{i+1}, \psi_{i+1}, w_i, \vartheta_i, w_{i+1}, \vartheta_{i+1}]^T. \quad (3)$$

The FE matrices have structure [1]

$$\mathbf{M}^{(e)} = \rho \begin{bmatrix} \mathbf{S}_1^{-T} (A \mathbf{I}_\Phi + J \mathbf{I}_{\Phi'}) \mathbf{S}_1^{-1} & \mathbf{0} \\ \mathbf{0} & \mathbf{S}_2^{-T} (A \mathbf{I}_\Phi + J \mathbf{I}_{\Phi'}) \mathbf{S}_2^{-1} \end{bmatrix}, \quad (4)$$

$$\mathbf{G}^{(e)} = 2 \rho J \begin{bmatrix} \mathbf{0} & \mathbf{S}_1^{-T} \mathbf{I}_{\Phi'} \mathbf{S}_2^{-1} \\ -\mathbf{S}_2^{-T} \mathbf{I}_{\Phi'} \mathbf{S}_1^{-1} & \mathbf{0} \end{bmatrix}, \quad (5)$$

$$\mathbf{K}^{(e)} = E J \begin{bmatrix} \mathbf{S}_1^{-T} \mathbf{I}_{\Phi''} \mathbf{S}_1^{-1} & \mathbf{0} \\ \mathbf{0} & \mathbf{S}_2^{-T} \mathbf{I}_{\Phi''} \mathbf{S}_2^{-1} \end{bmatrix},$$

where

$$\mathbf{I}_\Phi = \int_0^l \Phi^T(x) \Phi(x) dx, \quad \mathbf{I}_{\Phi'} = \int_0^l \Phi'^T(x) \Phi'(x) dx, \quad \mathbf{I}_{\Phi''} = \int_0^l \Phi''^T(x) \Phi''(x) dx,$$

$$\Phi(x) = [1, x, x^2, x^3], \quad \mathbf{S}_{1,2} = \begin{bmatrix} 1 & 0 & 0 & 0 \\ 0 & \pm 1 & 0 & 0 \\ 1 & l & l^2 & l^3 \\ 0 & \pm 1 & \pm 2l & \pm 3l^2 \end{bmatrix}, \quad \text{sign + for } \mathbf{S}_1, \quad \text{sign - for } \mathbf{S}_2$$

and symbol $-T$ designates a matrix inversion of the transposed matrix ($\mathbf{S}_i^{-T} = (\mathbf{S}_i^T)^{-1}$, $i = 1, 2$). Every shaft element of length l is determined by mass density ρ , cross-section area A , second moment of cross-section area J and Young's modulus E .

External damping forces, acting on the shaft FE, depend on the lateral absolute velocity. The Rayleigh dissipation function in the inertial coordinate system X, Y, Z is expressed as

$$R_E^{(e)} = \frac{1}{2} \int_0^l [b_{EY} \dot{v}^2(x, t) + b_{EZ} \dot{w}^2(x, t)] dx, \quad (6)$$

where b_{EY} and b_{EZ} [$\text{kg m}^{-1} \text{s}^{-1}$] are coefficients of viscous damping per unit length of the shaft FE. Its lateral deformations along the shaft FE are approximated by polynomial function in the form

$$v(x, t) = \Phi(x) \mathbf{S}_1^{-1} [v_i, \psi_i, v_{i+1}, \psi_{i+1}]^T, \quad w(x, t) = \Phi(x) \mathbf{S}_2^{-1} [w_i, \vartheta_i, w_{i+1}, \vartheta_{i+1}]^T. \quad (7)$$

The external damping matrix $\mathbf{B}_E^{(e)}$ results from identity

$$\frac{\partial R_E^{(e)}}{\partial \dot{\mathbf{q}}_{YZ}^{(e)}} = \mathbf{B}_E^{(e)} \dot{\mathbf{q}}_{YZ}^{(e)}, \quad \mathbf{B}_E^{(e)} = \begin{bmatrix} b_{EY} \mathbf{S}_1^{-T} \mathbf{I}_\Phi \mathbf{S}_1^{-1} & \mathbf{0} \\ \mathbf{0} & b_{EZ} \mathbf{S}_2^{-T} \mathbf{I}_\Phi \mathbf{S}_2^{-1} \end{bmatrix}. \quad (8)$$

The normal stress σ_I generated by internal damping forces in axial direction can be expressed as proportional to longitudinal strain velocity [2] in the form $\sigma_I = b_I E \dot{\varepsilon}_x$, where b_I [s] is coefficient of viscous internal damping and ε_x is longitudinal unit deformation. The power of the elementary damping force transmitted by surface element dA of cross-section is $\sigma_I dA \dot{\varepsilon}_x dx$, where $\dot{\varepsilon}_x dx$ is strain rate. The corresponding Rayleigh dissipation function in rotating coordinate system x, y, z ($x \equiv X$) is expressed as

$$R_I^{(e)} = \frac{1}{2} \int_0^l \int_A b_I E \dot{\varepsilon}_x^2 dA dx. \quad (9)$$

Providing small angular flexural cross-section displacements longitudinal unit deformation in arbitrary point (η, ζ) of shaft cross-section is

$$\varepsilon_x = -\eta \frac{\partial^2 v_r}{\partial x^2} - \zeta \frac{\partial^2 w_r}{\partial x^2}. \quad (10)$$

The lateral shaft FE deformations v_r, w_r in the rotating coordinate frame x, y, z can be approximated in the similar form to (7). The *internal damping matrix* $\mathbf{B}_I^{(e)}$ results from identity

$$\frac{\partial R_I^{(e)}}{\partial \dot{\mathbf{q}}_{yz}} = \mathbf{B}_I^{(e)} \dot{\mathbf{q}}_{yz}^{(e)}, \quad (11)$$

where shaft FE displacements in rotating coordinate system are arranged into vector

$$\mathbf{q}_{yz}^{(e)} = [v_{i,r}, \psi_{i,r}, v_{i+1,r}, \psi_{i+1,r}, w_{i,r}, \vartheta_{i,r}, w_{i+1,r}, \vartheta_{i+1,r}]^T. \quad (12)$$

According to (9) up to (12) we get internal damping matrix in the rotating coordinate system

$$\mathbf{B}_I^{(e)} = b_I E J \begin{bmatrix} \mathbf{S}_1^{-T} \mathbf{I}_{\Phi''} \mathbf{S}_1^{-1} & \mathbf{0} \\ \mathbf{0} & \mathbf{S}_2^{-T} \mathbf{I}_{\Phi''} \mathbf{S}_2^{-1} \end{bmatrix}. \quad (13)$$

We use the relations

$$\mathbf{q}_{yz}^{(e)} = \mathbf{T}(t) \mathbf{q}_{YZ}^{(e)}, \quad \mathbf{T}(t) = \begin{bmatrix} \mathbf{E} \cos \omega t & \mathbf{D} \sin \omega t \\ -\mathbf{D} \sin \omega t & \mathbf{E} \cos \omega t \end{bmatrix}, \quad \mathbf{D} = \text{diag}[1, -1, 1, -1] \quad (14)$$

between the displacement vectors of shaft FE nodal points in the rotating x, y, z and the inertial X, Y, Z coordinate systems. Mathematical model of the shaft FE bending vibration according to (2), (8) and after transformation of the internal damping force vector $(\mathbf{f}_I^{(e)})_{YZ} = -\mathbf{B}_I^{(e)} \dot{\mathbf{q}}_{yz}^{(e)}$ into the inertia coordinate system, has the form

$$\mathbf{M}^{(e)} \ddot{\mathbf{q}}_{YZ}^{(e)} + (\mathbf{B}_E^{(e)} + \mathbf{B}_I^{(e)} + \omega \mathbf{G}^{(e)}) \dot{\mathbf{q}}_{YZ}^{(e)} + (\mathbf{K}^{(e)} + \omega \mathbf{C}^{(e)}) \mathbf{q}_{YZ}^{(e)} = \mathbf{0}, \quad (15)$$

where so-called circulatory matrix

$$\omega \mathbf{C}^{(e)} = \omega b_I E J \begin{bmatrix} \mathbf{0} & \mathbf{S}_1^{-T} \mathbf{I}_{\Phi''} \mathbf{S}_1^{-1} \mathbf{D} \\ -\mathbf{D} \mathbf{S}_1^{-T} \mathbf{I}_{\Phi''} \mathbf{S}_1^{-1} & \mathbf{0} \end{bmatrix}, \quad (16)$$

for constant angular rotor velocity ω is in time the constant skew symmetric matrix.

3. Equations of rotor motion

The motion equations of the automotive turbocharger, including the rotor shaft, turbine wheel, compressor wheel, seal and thrust rings and two rotating floating ring bearings (Fig. 1), will be derived in the configuration space

$$\mathbf{q} = [\mathbf{q}_R^T, \mathbf{q}_B^T]^T = [\dots, v_i, w_i, \vartheta_i, \psi_i, \dots, v_{R_a}, w_{R_a}, v_{R_b}, w_{R_b}]^T. \quad (17)$$

The vector \mathbf{q}_R of dimension $4N$ (N = number of rotor shaft nodal points) was defined in (1) and the sub-vector

$$\mathbf{q}_B = [v_{R_a}, w_{R_a}, v_{R_b}, w_{R_b}]^T \quad (18)$$

expresses lateral displacements of the rigid bearing rings R_a (left) and R_b (right) with respect to frame. The matrices of the shaft element defined in equation (15) must be transformed in the form

$$\mathbf{X}_e = \mathbf{P}^T \mathbf{X}^{(e)} \mathbf{P}, \quad \mathbf{X}^{(e)} = \mathbf{M}^{(e)}, \mathbf{B}_E^{(e)}, \mathbf{B}_I^{(e)}, \mathbf{G}^{(e)}, \mathbf{K}^{(e)}, \mathbf{C}^{(e)}, \quad (19)$$

where permutation matrix \mathbf{P} corresponds to relation

$$\mathbf{q}_{YZ}^{(e)} = \mathbf{P} \mathbf{q}_e, \quad \mathbf{q}_e = [v_i, w_i, \vartheta_i, \psi_i, v_{i+1}, w_{i+1}, \vartheta_{i+1}, \psi_{i+1}]^T.$$

The structure of the all global rotor shaft matrices without disks and bearings is given by following scheme

$$\mathbf{X}_R = \sum_e \text{diag}[\mathbf{0}, \mathbf{X}_e, \mathbf{0}], \quad \mathbf{X}_R = \mathbf{M}_R, \mathbf{B}_R^{(E)}, \mathbf{B}_R^{(I)}, \mathbf{G}_R, \mathbf{K}_R, \mathbf{C}_R \in R^{4N, 4N} \quad (20)$$

with block matrices \mathbf{X}_e determined in (19).

The mass \mathbf{M}_D , gyroscopic $\omega \mathbf{B}_D$ and external damping \mathbf{B}_D matrices of the axisymmetric rigid disk firmly linked with the rotor shaft in nodal point i can be derived using Lagrange's approach based on the kinetic energy E_D and dissipation function R_D . The mass, external damping and gyroscopic matrices of the rotor shaft with disks (turbine and compressor wheels, seal and trust rings) have structure

$$\mathbf{X}_R = \sum_e \text{diag}[\mathbf{0}, \mathbf{X}_e, \mathbf{0}] + \sum_D \mathbf{X}_D, \quad \mathbf{X}_R = \mathbf{M}_R, \mathbf{B}_R^{(E)}, \mathbf{G}_R, \quad \mathbf{X}_D = \mathbf{M}_D, \mathbf{B}_D, \mathbf{G}_D, \quad (21)$$

where \mathbf{X}_e are the shaft FE matrices (19) and the disk matrices are localized on positions corresponding to coupling shaft nodal points displacements.

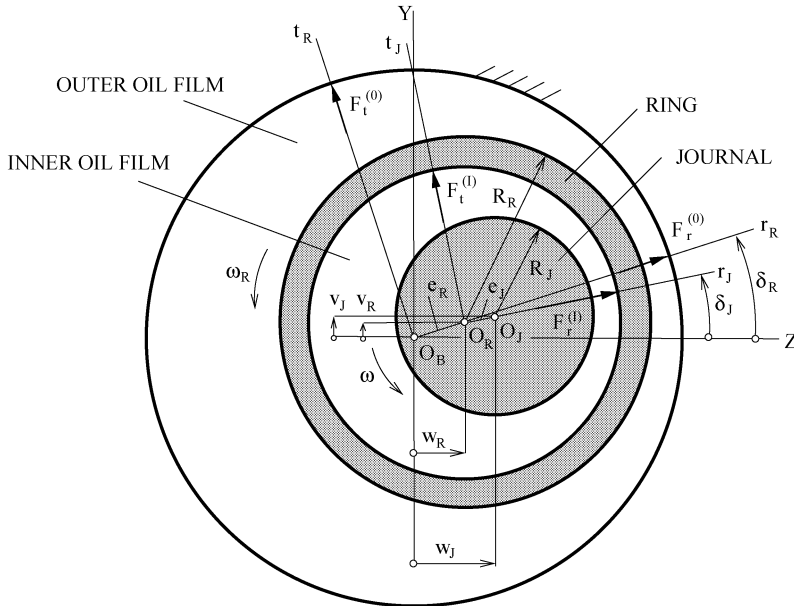


Fig.3: Rotating floating ring bearing

In order to reduce the bearing friction, the high-speed turbocharger is supported on the rotating floating ring bearings having the inner (I) and outer (O) oil films (Fig. 3). We consider the rotor shaft rotation with constant angular velocity ω in the opposite direction around X axis. Using Lagrange's approach we derive, on condition lateral ring vibrations, the mass matrix of the rotating floating ring bearings

$$\mathbf{M}_B = \text{diag}[m_a, m_a, m_b, m_b], \quad (22)$$

where m_a, m_b are ring masses. The bearing forces $F_r^{(I)}, F_t^{(I)}$ and $F_r^{(O)}, F_t^{(O)}$ (see Fig. 3) are based on the corresponding rotating coordinate system [4] r_J, t_J and r_R, t_R of the journal (J) and ring (R).

In case of linear rotordynamics the bearing forces $F_r^{(I)}, F_t^{(I)}$ and $F_r^{(O)}, F_t^{(O)}$ are linearized in the neighbourhood of the static equilibrium position. In case of the floating ring bearings the linearized forces in the inertial coordinate system are

$$\begin{bmatrix} F_Y^{(I)} \\ F_Z^{(I)} \end{bmatrix} = \begin{bmatrix} F_{0,Y}^{(I)} \\ F_{0,Z}^{(I)} \end{bmatrix} - \begin{bmatrix} k_{YY}(\omega) & k_{YZ}(\omega) \\ k_{ZY}(\omega) & k_{ZZ}(\omega) \end{bmatrix} \begin{bmatrix} \bar{v}_J - \bar{v}_R \\ \bar{w}_J - \bar{w}_R \end{bmatrix} - \begin{bmatrix} b_{YY}(\omega) & b_{YZ}(\omega) \\ b_{ZY}(\omega) & b_{ZZ}(\omega) \end{bmatrix} \begin{bmatrix} \dot{v}_J - \dot{v}_R \\ \dot{w}_J - \dot{w}_R \end{bmatrix}, \quad (23)$$

$$\begin{bmatrix} F_Y^{(O)} \\ F_Z^{(O)} \end{bmatrix} = \begin{bmatrix} F_{0,Y}^{(O)} \\ F_{0,Z}^{(O)} \end{bmatrix} - \begin{bmatrix} k_{YY}(\omega) & k_{YZ}(\omega) \\ k_{ZY}(\omega) & k_{ZZ}(\omega) \end{bmatrix} \begin{bmatrix} \bar{v}_R \\ \bar{w}_R \end{bmatrix} - \begin{bmatrix} b_{YY}(\omega) & b_{YZ}(\omega) \\ b_{ZY}(\omega) & b_{ZZ}(\omega) \end{bmatrix} \begin{bmatrix} \dot{v}_R \\ \dot{w}_R \end{bmatrix}, \quad (24)$$

where \bar{v}_J, \bar{w}_J and \bar{v}_R, \bar{w}_R are displacements of the journal and ring centres from the static equilibrium position resulted from static load of the journals and bearing rings.

As a result of specific ring speed ratio $RSR = \omega_R/\omega$ [6] in steady-state conditions (constant ω) the stiffness and damping matrices of the inner and outer oil-films in Eqs. (23) and (24) depend on ω . We describe them as $\mathbf{K}_x^{(I)}(\omega), \mathbf{B}_x^{(I)}(\omega)$ for inner oil-film and $\mathbf{K}_x^{(O)}(\omega), \mathbf{B}_x^{(O)}(\omega)$ for outer oil-film of the left ($x = a$) and right ($x = b$) bearings. The changes of the bearing forces, relating to small displacements and velocities of the rotor from static equilibrium position, can be expressed by the second and the third components on the right side in Eqs. (23) and (24). They can be expressed in the matrix form

$$\Delta \mathbf{f}_B = -\mathbf{K}_B(\omega) \begin{bmatrix} \bar{\mathbf{q}}_R \\ \bar{\mathbf{q}}_B \end{bmatrix} - \mathbf{B}_B(\omega) \begin{bmatrix} \dot{\bar{\mathbf{q}}}_R \\ \dot{\bar{\mathbf{q}}}_B \end{bmatrix}, \quad (25)$$

where $\bar{\mathbf{q}}_R, \bar{\mathbf{q}}_B$ are vectors of rotor shaft and bearing rings displacements from the static equilibrium position. According to (23) and (24), the stiffness and damping matrices of the two separated oil-films of both bearings are localized in global matrices according to vectors $\bar{\mathbf{q}}_{J_x} = [\bar{v}_{J_x}, \bar{w}_{J_x}]^T, \bar{\mathbf{q}}_{R_x} = [\bar{v}_{R_x}, \bar{w}_{R_x}]^T, x = a, b$ as follows

$$\mathbf{K}_B(\omega) = \begin{bmatrix} \mathbf{K}_a^{(I)} & & -\mathbf{K}_a^{(I)} & \\ & \mathbf{K}_b^{(I)} & & -\mathbf{K}_b^{(I)} \\ -\mathbf{K}_a^{(I)} & & \mathbf{K}_a^{(I)} + \mathbf{K}_a^{(O)} & \\ & -\mathbf{K}_b^{(I)} & & \mathbf{K}_b^{(I)} + \mathbf{K}_b^{(O)} \end{bmatrix} \begin{Bmatrix} \bar{\mathbf{q}}_{J_a} \\ \bar{\mathbf{q}}_{J_b} \\ \bar{\mathbf{q}}_{R_a} \\ \bar{\mathbf{q}}_{R_b} \end{Bmatrix}, \quad \mathbf{B}_B(\omega) \sim \mathbf{K}_B(\omega). \quad (26)$$

The linearized motion equations of the turbochargers (Fig.1), according to (21),(22) and (25), can be written as

$$\begin{bmatrix} \mathbf{M}_R & \mathbf{0} \\ \mathbf{0} & \mathbf{M}_B \end{bmatrix} \begin{bmatrix} \ddot{\bar{\mathbf{q}}}_R \\ \ddot{\bar{\mathbf{q}}}_B \end{bmatrix} + \left(\begin{bmatrix} \mathbf{B}_R^{(E)} + \mathbf{B}_R^{(I)} - \omega \mathbf{G}_R & \mathbf{0} \\ \mathbf{0} & \mathbf{0} \end{bmatrix} + \mathbf{B}_B(\omega) \right) \begin{bmatrix} \dot{\bar{\mathbf{q}}}_R \\ \dot{\bar{\mathbf{q}}}_B \end{bmatrix} + \left(\begin{bmatrix} \mathbf{K}_R - \omega \mathbf{C}_R & \mathbf{0} \\ \mathbf{0} & \mathbf{0} \end{bmatrix} + \mathbf{K}_B(\omega) \right) \begin{bmatrix} \bar{\mathbf{q}}_R \\ \bar{\mathbf{q}}_B \end{bmatrix} = \begin{bmatrix} \mathbf{f}_R(t) \\ \mathbf{0} \end{bmatrix}, \quad (27)$$

where $\mathbf{f}_R(t)$ is vector of the unbalance of disks (turbine and compressor wheels).

4. Application

The homogenous motion equations (27) (for $\mathbf{f}_R(t) = \mathbf{0}$) was applied on eigenvalues calculation of the small automotive turbocharger with rotor mass 0.1 [kg]. The rotor discretized into 13 nodes (Fig.1) is supported on two short cylindrical floating ring bearings. The eigenvalues λ_ν are found by solving the eigenvalue problem

$$(\mathbf{A} - \lambda \mathbf{E}) \mathbf{u} = \mathbf{0} \quad (28)$$

in state space $\mathbf{u} = [\dot{\mathbf{q}}, \mathbf{q}]^T$, where non-symmetric system matrix is

$$\mathbf{A} = \begin{bmatrix} -\mathbf{M}^{-1} \mathbf{B}(\omega) & -\mathbf{M}^{-1} \mathbf{K}(\omega) \\ \mathbf{E} & \mathbf{0} \end{bmatrix} \quad (29)$$

and \mathbf{M} , $\mathbf{B}(\omega)$, $\mathbf{K}(\omega)$ are global matrices of order $n = 56$ in the motion equations (27). The bearing stiffness and damping coefficients were calculated for the concrete oil and geometrical bearing parameters by means of bearing dimensionless stiffness κ_{ij} and damping β_{ij} coefficients [4], [6] using the Reynolds lubrication equation for radial cylindrical short bearings with the non-cavitating oil-films.

The linearized mathematical model of the rotor has besides complex conjugate pairs of eigenvalues also even number of real values representing nonoscillatory overdamping modes. The Campbell diagram displayed at Fig.4 expresses the dependence of the eigenfrequencies (imaginary parts of the complex eigenvalues) of the turbocharger on rotor speed $n = 30 \omega / \pi$ [rpm]. The critical speeds n_k [rpm], where the eigenfrequencies cuts the synchronous excitation line, can be calculated as roots of the nonlinear equation

$$n = \frac{30}{\pi} \text{Im}\{\lambda_\nu(n)\} . \quad (30)$$

The calculated critical speeds in the investigated rotor speed range $n \in (20000, 240000)$ [rpm] are given in Table 1.

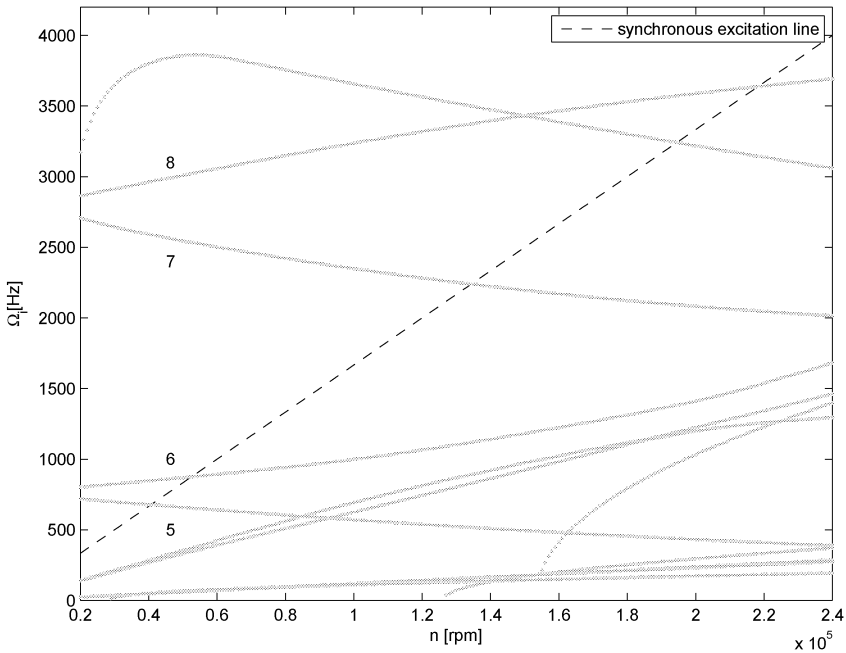


Fig.4: Campbell diagram of the turbocharger

Critical speeds					
order	without strengthening		with strengthening		
	f [Hz]	n [rpm]	f [Hz]	n [rpm]	
1	677.38	40643	712.94	42776	B
2	875.20	52512	889.71	53377	F
3	2239.38	134363	2483.76	149026	B
4	3241.25	194475	4865.54	291932	B
5	3637.61	218257	5436.85	326211	F

Tab.1: Critical speed of the rotor (B=backward, F=forward) without and with strengthening of the shaft in area of the compressor wheel

5. Conclusion

The described method was applied to investigate the complex eigenvalues, stability and critical speeds of the well-balanced concrete turbocharger rotor supported on two floating ring bearings. The computer program in MATLAB code makes it possible to analyse an influence of design and operation parameters of the turbochargers on these phenomena. The adjusted nonlinear mathematical model including nonlinear characteristics of the bearing forces will be used for vibration analysis at the large journals and floating bearing rings deflections.

Acknowledgement

This work was supported by the European Regional Development Fund (ERDF), project ‘NTIS’, European Centre of Excellence, CZ.1.05/1.1.00/02.0090.

References

- [1] Byrtus M., Hajžman M., Zeman V.: *Dynamika rotujících soustav*, Monograph, UWB, Pilsen 2010
- [2] Gash R., Pfützner H.: *Rotordynamik*, Springer, Berlin 1975
- [3] Genta G.: *Dynamics of Rotating Systems*, Springer, Heidelberg 2005
- [4] Krämer E.: *Dynamics of Rotors and Foundations*, Springer, Berlin 1993
- [5] Muszińska A.: *Rotordynamics*, CRC Press Taylor & Francis, Boca Raton 2005
- [6] Shäfer H.N.: *Rotordynamics of Automotive Turbochargers*, Springer, Heidelberg 2012
- [7] Yamamoto T., Ishida Y.: *Linear and Nonlinear Rotordynamics*, John Wiley & Sons, New York 2001

Received in editor's office: June 12, 2013

Approved for publishing: November 27, 2013